
End-to-End Multi-Task Denoising for joint SDR and PESQ Optimization

Jaeyoung Kim¹ Mostafa El-Kharmy¹ Jungwon Lee¹

Abstract

Supervised learning based on a deep neural network recently has achieved substantial improvement on speech enhancement. Denoising networks learn mapping from noisy speech to clean one directly, or to a spectra mask which is the ratio between clean and noisy spectrum. In either case, the network is optimized by minimizing mean square error (MSE) between predefined labels and network output of spectra or time-domain signal. However, existing schemes have either of two critical issues: spectra and metric mismatches. The spectra mismatch is a well known issue that any spectra modification after short-time Fourier transform (STFT), in general, cannot be fully recovered after inverse STFT. The metric mismatch is that a conventional MSE metric is sub-optimal to maximize our target metrics, signal-to-distortion ratio (SDR) and perceptual evaluation of speech quality (PESQ). This paper presents a new end-to-end denoising framework with the goal of joint SDR and PESQ optimization. First, the network optimization is performed on the time-domain signals after ISTFT to avoid spectra mismatch. Second, two loss functions which have improved correlations with SDR and PESQ metrics are proposed to minimize metric mismatch. The experimental result showed that the proposed denoising scheme significantly improved both SDR and PESQ performance over the existing methods.

not learn any model architecture from data but they provide blind signal estimation based on their predefined speech and noise models. However, their model assumptions, in general, do not match with real-world complex non-stationary noise, which often leads to failure of noise estimation and tracking. On the contrary, a neural network directly learns nonlinear complex mapping from noisy speech to clean one only by referencing data without any prior assumption. With more number of data, a neural network can learn better underlying mapping.

Spectra mask estimation is a popular supervised denoising method that predicts a time-frequency spectra mask to obtain an estimate of clean speech by multiplication with noisy spectra. There are numerous types of spectra mask estimation depending on how to define mask labels. For example, the author in (Narayanan & Wang, 2013) proposed ideal binary mask (IBM) as a training label, where it is set to be zero or one depending on the signal to noise ratio (SNR) of a noisy spectra. Ideal ratio mask (IRM) (Wang et al., 2014) and ideal magnitude mask (IAM) (Erdogan et al., 2015) provided non-binary soft mask labels to overcome coarse label mapping of IBM. Phase sensitive mask (PSM) (Erdogan et al., 2015) considers spectra phase difference between clean and noisy signal in order to correctly maximize signal to noise ratio (SNR).

Generative models such as generative adversarial networks (GANs) and variational autoencoders (VAEs) suggested an alternative to supervised learning. In speech enhancement GAN (SEGAN) (Pascual et al., 2017), a generator network is trained to output a time-domain denoised signal that can fool a discriminator from a true clean signal. TF-SEGAN (Soni et al., 2018) extended SEGAN into time-frequency spectra. (Bando et al., 2018), on the other hand, combined a VAE-based speech model with an non-negative matrix factorization (NMF) for noise spectra to show good performance on unseen data.

However, all the schemes described above suffer from either of two critical issues: metric and spectra mismatches. SDR and PESQ are two most widely known metrics for measuring quality of speech signal. The typical mean square error (MSE) criterion popularly used for spectra mask estimation is not optimal to maximize our target metrics of SDR

1. Introduction

In recent years, deep neural networks have shown great success in speech enhancement compared with traditional statistical approaches. Statistical enhancement schemes such as MMSE STSA (Ephraim & Malah, 1984) and OMLSA (Ephraim & Malah, 1985; Cohen & Berdugo, 2001) do

¹Samsung Semiconductor Incorporated, USA. Correspondence to: Jaeyoung Kim <jaeyl.kim@samsung.com>.

and PESQ. For example, decreasing mean square error of noisy speech signal often degrades SDR or PESQ due to different weighting on frequency components or non-linear transforms involved in the metric. Furthermore, GAN-based generative models don't have even a specific loss function to minimize. Although they are robust for unseen data, they typically perform much worse for test data with small data mismatch. The spectra mismatch is a well known issue that any spectra modification after short-time Fourier transform (STFT), in general, cannot be fully recovered after inverse STFT. Therefore, spectra mask estimation and other alternatives optimized in the spectra domain always have a potential risk of performance loss.

This paper presents a new end-to-end multi-task denoising scheme. First, the proposed framework presents two loss functions:

- SDR loss function: instead of typical MSE, SDR metric is used as a loss function. The scale-invariant term in SDR metric is incorporated as a part of training, which provided significant SDR boost.
- PESQ loss function: PESQ metric is redesigned to be usable as a loss function. The two key variables of PESQ, symmetric and asymmetric disturbances are approximated to be optimized during training.

The proposed multi-task denoising scheme combines two loss functions for joint SDR and PESQ optimization. Second, a denoising network still predicts a time-frequency mask but the network optimization is performed after ISTFT in order to avoid spectra mismatch. SDR loss function is naturally calculated from the time-domain reconstructed signal. PESQ loss function needs spectra powers for disturbance calculation and therefore, the second STFT is applied on the time-domain signal for spectra consistency. The evaluation result showed that the proposed framework provided large improvement both on SDR and PESQ.

2. Background and Related Works

Figure 1 illustrates the overall speech denoising flow. The input noisy signal is given by

$$y^u(n) = x^u(n) + n^u(n) \quad (1)$$

where u is a utterance index, n is a time index, $x^u(n)$ is clean speech and $n^u(n)$ is noise signal. $Y_{m,k}^u$ is STFT output, where m and k are frame and frequency indices, respectively. It is fed into two separate paths. For the upper path, the magnitude of $Y_{m,k}^u$ is passed to the Denoiser block. On the contrary, the phase of $Y_{m,k}^u$ is bypassed without compensation. $\hat{Y}_{m,k}^u$ is synthesized by noisy input phase and denoised spectra amplitude. After ISTFT, we can recover time-domain denoised output $\hat{y}^u(n)$.

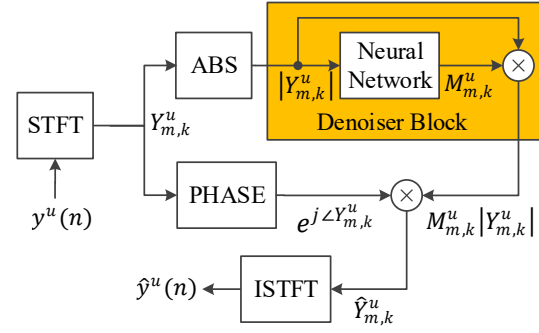


Figure 1. Block Diagram of Denoising Framework

2.1. Spectra Mask Estimation

The neural network in Figure 1 predicts a time-frequency mask to obtain an estimate of the clean spectra amplitude. The estimated mask is multiplied by the input spectra amplitude as follows:

$$|\hat{Y}_{m,k}^u| = M_{m,k}^u |Y_{m,k}^u| \quad (2)$$

Given clean and noisy spectra amplitude pairs, the mask estimation is to minimize a predefined distance measure, d for all utterances and time-frequency bins:

$$L = \min_{\phi} \sum_{u=1}^U \sum_{m=1}^{M_u} \sum_{k=1}^K d(M_{m,k}^u, |X_{m,k}^u|, |Y_{m,k}^u|) \quad (3)$$

where ϕ is a denoiser parameter, M_u is the number of frames for the utterance u , K is the number of frequency bins, d is a distortion metric, $|X_{m,k}^u|$ is spectra amplitude of clean speech and $|Y_{m,k}^u|$ is spectra amplitude of noisy speech. Ideal binary mask (IBM) and ideal ratio mask (IRM) are two well-known mask labels given by

$$L_{\text{IBM},m,k}^u = \begin{cases} 1, & \text{if } \frac{|X_{m,k}^u|}{|N_{m,k}^u|} \geq 10^{\frac{S_{th,k}}{10}} \\ 0, & \text{else} \end{cases} \quad (4)$$

where $S_{th,k}$ is a log-scale threshold for frequency index k .

$$L_{\text{IRM},m,k}^u = \frac{|X_{m,k}^u|}{|X_{m,k}^u| + |N_{m,k}^u|} \quad (5)$$

The distortion metric for IBM and IRM is given by

$$d_1(M_{m,k}^u, |X_{m,k}^u|, |N_{m,k}^u|) = (M_{m,k}^u - L_{x,m,k}^u)^2 \quad (6)$$

where x is either IBM or IRM. The one issue for two mask labels is that they don't correctly recover clean speech. For example, $L_{x,m,k}^u |Y_{m,k}^u|$ is generally not equal to $|X_{m,k}^u|$. Ideal amplitude mask (IAM) is defined to represent the exact magnitude ratio:

$$L_{\text{IAM},m,k}^u = \frac{|X_{m,k}^u|}{|X_{m,k}^u| + |N_{m,k}^u|} \quad (7)$$

For IAM, instead of the distortion metric in Eq.(6), (Weninger et al., 2014) suggested spectra magnitude minimization, which was shown to have significant improvement:

$$d_2(M_{m,k}^u, |X_{m,k}^u|, |Y_{m,k}^u|) = (M_{m,k}^u |Y_{m,k}^u| - |X_{m,k}^u|)^2 \quad (8)$$

The one drawback in Eq.(8) is that it cannot correctly maximize signal to noise ratio (SNR) when phase difference between clean and noisy spectra is not zero. The optimal distortion measure to maximize SNR is to minimize mean square error between complex spectra as follows:

$$d_3(M_{m,k}^u, |X_{m,k}^u|, |Y_{m,k}^u|, \angle X_{m,k}^u, \angle Y_{m,k}^u) = \left| M_{m,k}^u |Y_{m,k}^u| e^{j\angle Y_{m,k}^u} - |X_{m,k}^u| e^{j\angle X_{m,k}^u} \right|^2 \quad (9)$$

Eq.(9) can be rearranged after removing unnecessary terms for optimization:

$$d_3(M_{m,k}^u, |X_{m,k}^u|, |Y_{m,k}^u|, \angle X_{m,k}^u, \angle Y_{m,k}^u) = (M_{m,k}^u |Y_{m,k}^u| - |X_{m,k}^u| \cos(\angle Y_{m,k}^u - \angle X_{m,k}^u))^2 \quad (10)$$

The equivalent mask label, called phase sensitive mask (PSM) is given by

$$L_{\text{PSM},m,k}^u = \frac{|X_{m,k}^u|}{|X_{m,k}^u| + N_{m,k}^u} \cos(\angle Y_{m,k}^u - \angle X_{m,k}^u) \quad (11)$$

In this paper, PSM (Erdogan et al., 2015) was chosen as a baseline denoising scheme because PSM showed the best performance on the target metrics of SDR and PESQ among spectra mask estimation schemes.

2.2. Griffin-Lim Algorithm

ISTFT operation in Figure 1 consists of IFFT, windowing and overlap addition as follows:

$$\hat{y}^u(n) = \sum_{m=0}^{M_u-1} \hat{y}_m^u(n - m\delta) w(n - m\delta) \quad (12)$$

where δ is frame shifting number and $\hat{y}_m^u(n)$ is IFFT of $\hat{Y}_{m,k}^u$. Due to the overlapped frame sequence generation, any arbitrary spectra modification can cause spectra mismatch. For example, $\hat{Y}_{m,k}^u$ is, in general, not matched to the STFT of $\hat{y}^u(n)$ due to the modification of spectra amplitude. Griffin-Lim algorithm (Griffin & Lim, 1984) is to find legitimate $z^u(n)$, which has the closest spectra to $\hat{Y}_{m,k}^u$. A legitimate signal is meant to have no spectra mismatch. The Griffin-Lim formulation is given by

$$\min_{z^u(n)} \sum_{n=0}^{N-1} \sum_{m=0}^{M_u-1} (\hat{y}_m^u(n) - z^u(n) w(n - m\delta))^2 \quad (13)$$

The solution can be easily derived by finding $z^u(n)$ that makes Eq.(13) have zero gradient:

$$z^u(n) = \frac{\sum_{m=0}^{M_u-1} w(n - m\delta) \hat{y}_m^u(n - m\delta)}{\sum_{m=0}^{M_u-1} w^2(n - m\delta)} \quad (14)$$

Although Griffin-Lim algorithm guarantees to find a legitimate signal with minimum MSE, it is still not guaranteed to coincide with $\hat{Y}_{m,k}^u$. The iterative Griffin-Lim algorithm further decreases spectra magnitude mismatch for every iteration by allowing phase distortion, which will be evaluated in conjunction with the proposed framework.

3. The Proposed Framework

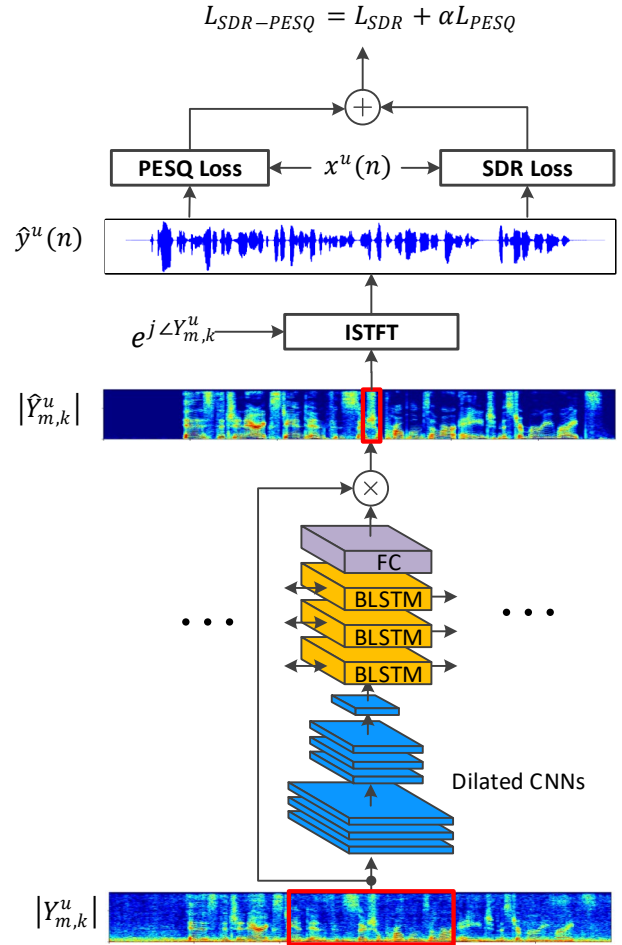


Figure 2. Illustration of End-to-End Multi-Task Denoising based on CNN-BLSTM

Figure 2 describes the proposed end-to-end multi-task denoising framework. The underlying model architecture is composed of convolution layers and bi-directional BLSTMs. The spectrogram formed by 11 frames of the noisy spectra

amplitude $|Y_{m,k}^u|$ is the input to the convolutional layers with the kernel size of 5×5 . The dilated convolution with rate of 2 and 4 is applied to the second and third layers, respectively, in order to increase kernel's coverage on frequency bins. Dilation is only applied to the frequency dimension because time correlation will be learned by bi-directional LSTMs. Griffin-Lim ISTFT is applied to the synthesized complex spectra $\hat{Y}_{m,k}^u$ to obtain time-domain denoised output $\hat{y}^u(n)$. Two proposed loss functions are evaluated based on $\hat{y}^u(n)$ and therefore, they are free from spectra mismatch.

3.1. SDR Loss Function

Unlike SNR, the definition of SDR is not unique. There are at least two popularly used SDR definitions. The most well known Vincent's definition (Vincent et al., 2006) is given by

$$\text{SDR} = 10 \log_{10} \frac{\|x_{\text{target}}\|^2}{\|e_{\text{noise}} + e_{\text{artif}}\|^2} \quad (15)$$

There was an e_{interf} term in the original SDR but it is removed because there is no interference error for single source denoising problem. x_{target} and e_{noise} can be found by projecting denoised signal $\hat{y}^u(n)$ into clean and noise signal domain, respectively. e_{artif} is a residual term and they can be formulated as follows:

$$x_{\text{target}} = \frac{x^T \hat{y}}{\|x\|^2} x \quad (16)$$

$$e_{\text{noise}} = \frac{n^T \hat{y}}{\|n\|^2} n \quad (17)$$

$$e_{\text{artif}} = \hat{y} - \left(\frac{x^T \hat{y}}{\|x\|^2} x + \frac{n^T \hat{y}}{\|n\|^2} n \right) \quad (18)$$

Substituting Eq.(16), (17) and (18) into Eq.(15), the rearranged SDR is given by

$$\begin{aligned} \text{SDR} &= 10 \log_{10} \frac{\| \frac{x^T \hat{y}}{\|x\|^2} x \|^2}{\| \frac{x^T \hat{y}}{\|x\|^2} x - \hat{y} \|^2} \\ &= 10 \log_{10} \frac{\|\alpha x\|^2}{\|\alpha x - \hat{y}\|^2} \end{aligned} \quad (19)$$

where $\alpha = \arg \min_{\alpha} \|\alpha x - y\|$. Eq.(19) coincides with SI-SDR that is another popularly used SDR definition (Roux et al., 2018). In the general multiple source problems, they do not match each other. However, for our single source denoising problem, we can use them interchangeably without any confusion.

SDR loss function is defined as mini-batch average of Eq.(19):

$$L_{\text{SDR}} = \frac{1}{B} \sum_{u=0}^{B-1} 10 \log_{10} \frac{\|\alpha x^u\|^2}{\|\alpha x^u - \hat{y}^u\|^2} \quad (20)$$

Compared with conventional MSE loss function, scale-invariant α is included as a training variable in Eq.(20). Figure 3 illustrates why training α is important to maximize the SDR metric. For two noisy signal y_1 and y_2 , they have the same SNR because they positioned at the same circle centered at the clean signal x . However, their SDRs are different. For y_1 , SDR is $\frac{\|\alpha_1 x\|^2}{\|\alpha_1 x - y_1\|^2}$, which is $\frac{\|x\|^2}{\|x - \beta_1 y_1\|^2}$ by geometry. By the same way, SDR for y_2 is $\frac{\|x\|^2}{\|x - \beta_2 y_2\|^2}$. Clearly, y_1 is better than y_2 in terms of SDR metric but MSE criterion cannot distinguish between them because they have the same SNR.

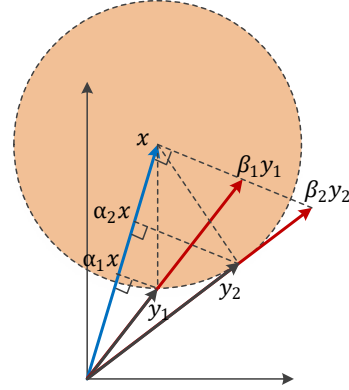


Figure 3. SDR comparison between two noisy signals with the same SNR

3.2. PESQ Loss Function

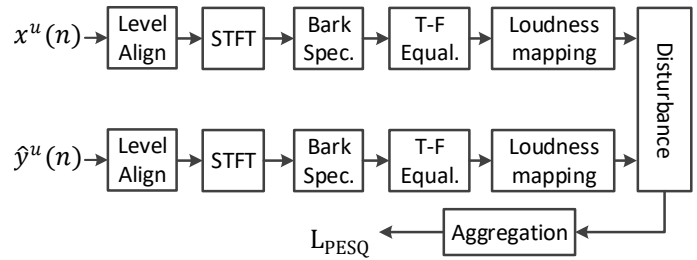


Figure 4. Block Diagram for L_{PESQ} : $x^u(n)$ is time-domain clean signal and $\hat{y}^u(n)$ is denoised time-domain signal after ISTFT.

Perceptual evaluation of speech quality (PESQ) (Rix et al., 2001) is ITU-T standard and it provides objective speech quality evaluation. Its value ranges from -0.5 to 4.5 and the higher PESQ means better perceptual quality. Although SDR and PESQ have high correlation, it is frequently observed that signal with smaller SDR have higher PESQ than the one with the higher SDR. For example, acoustic signal with high reverberation would have low SNR or SDR but

PESQ can be much better because time-frequency equalization in PESQ can compensate the most of channel fading effects. It is just one example and there are a lot of operations that make PESQ behave much differently from SDR. Therefore, SDR loss function cannot effectively optimize PESQ.

In this section, a new PESQ loss function is designed based on PESQ metric. Figure 4 shows the block diagram to find PESQ loss function L_{PESQ} . The overall procedure is similar to the PESQ system in (Rix et al., 2001). There are three major modifications. First, IIR filter in PESQ is removed. The reason is that time evolution of IIR filter is too deep to apply back-propagation. Second, delay adjustment routine is not necessary because training data pairs were already time-aligned. Third, bad-interval iteration was removed. PESQ improves metric calculations by detecting bad intervals of frames and updating metrics over those periods. As long as training clean and noisy data pairs are perfectly time-aligned, there's no significant impact on PESQ by removing this operation.

Level Alignment: The average power of clean and noisy speeches ranging from 300Hz to 3KHz are aligned to be 10^7 , which is a predefined power value. IIR filter gain 2.47 is also compensated in this block.

Bark Spectrum: Bark spectrum block is to find the mean of linear scale frequency bins according to the Bark scale mapping. The higher frequency bins are averaged with more number of bins, which effectively provides lower weighting to them. The mapped bark spectrum power can be formulated as follows:

$$B_{c,m,i}^u = \frac{1}{I_{i+1} - I_i} \sum_{k=I_i}^{I_{i+1}-1} |X_{m,k}^u|^2 \quad (21)$$

where I_i is the start of linear frequency bin number for the i^{th} bark spectrum, $B_{c,m,i}^u$ is i^{th} bark spectrum power of clean speech. All the positive linear frequency bins were mapped to 49 Bark spectrum bins. $B_{n,m,i}^u$ is a bark spectrum power of noisy speech and can be also found in the similar manner.

Time-Frequency Equalization: Each Bark spectrum bin of clean speech is compensated by the average power ratio between clean and noisy Bark spectrum as follows:

$$E_{c,m,i}^u = \frac{P_{n,i}^u + c_1}{P_{c,i}^u + c_1} B_{c,m,i}^u \quad (22)$$

where $P_{n,i}^u = \frac{1}{M_u} \sum_{m=0}^{M_u-1} B_{n,m,i}^u S_{n,m,i}^u$, $P_{c,i}^u = \frac{1}{M_u} \sum_{m=0}^{M_u-1} B_{c,m,i}^u S_{c,m,i}^u$, c_1 is a constant and $S_{n,m,i}^u$ and $S_{c,m,i}^u$ are silence masks that become 1 only when the corresponding bark spectrum power exceeds predefined thresholds. After frequency equalization, the short-term gain variation of a noisy bark spectrum is also compensated for each

frame:

$$S_m^u = \frac{G_{c,m}^u + c_2}{G_{n,m}^u + c_2} \quad (23)$$

$$S_m^u = 0.2S_{m-1}^u + 0.8S_m^u \quad (24)$$

$$E_{n,m,i}^u = S_m^u B_{n,m,i}^u \quad (25)$$

where $G_{n,m}^u = \sum_{i=0}^{I-1} B_{n,m,i}^u$, $G_{c,m}^u = \sum_{i=0}^{I-1} E_{c,m,i}^u$, I is the size of Bark spectrum bins, and c_2 is a constant.

Loudness Mapping: The power densities are transformed to a Soner loudness scale using Zwicker's law (Zwicker & Feldtkeller, 1967):

$$L_{x,m,i}^u = S_i \left(\frac{P_{0,i}}{0.5} \right) \left[\left(0.5 + 0.5 \frac{E_{x,m,i}^u}{P_{0,i}} \right) - 1 \right] \quad (26)$$

where $P_{0,i}$ is the absolute hearing threshold, S_i is the loudness scaling factor, and r is Zwicker power and x can be c (clean) or n (noisy).

Disturbance Processing: The raw disturbance is difference between clean and noisy loudness densities with following operations:

$$D_{m,i}^u = \max(L_{c,m,i}^u - L_{n,m,i}^u - \text{DZ}_{m,i}^u, 0) + \min(L_{c,m,i}^u - L_{n,m,i}^u + \text{DZ}_{m,i}^u, 0) \quad (27)$$

where $\text{DZ}_{m,i}^u = 0.25 \min(L_{c,m,i}^u, L_{n,m,i}^u)$. If absolute difference between clean and noisy loudness densities are less than 0.25 of minimum of two densities, raw disturbance becomes zero. From raw disturbance, symmetric frame disturbance is given by

$$\text{FD}_m^u = \sum_{i=0}^{I-1} w_i \sqrt{\frac{1}{\sum_{i=0}^{I-1} w_i} \sum_{i=0}^{I-1} (w_i D_{m,i}^u)^2} \quad (28)$$

where w_i is predefined weighting for bark spectrum bins. Asymmetric frame disturbance has additional scaling and thresholding steps as follows:

$$h_{m,i}^u = \left(\frac{B_{n,m,i}^u + 50}{B_{c,m,i}^u + 50} \right)^{1.2} \quad (29)$$

$$h_{m,i}^u = \begin{cases} 12, & \text{if } h_{m,i}^u > 12 \\ 0, & \text{if } h_{m,i}^u < 3 \end{cases} \quad (30)$$

$$\text{AFD}_m^u = \sum_{i=0}^{I-1} w_i \sqrt{\frac{1}{\sum_{i=0}^{I-1} w_i} \sum_{i=0}^{I-1} (w_i D_{m,i}^u h_{m,i}^u)^2} \quad (31)$$

Aggregation: PESQ loss function L_{PESQ} can be found as follows:

$$L_{\text{PESQ}} = 4.5 - 0.1d_{\text{sym}} - 0.0309d_{\text{asym}} \quad (32)$$

d_{sym} can be found from two stage averaging:

$$\text{PSQM}_s^u = \sqrt[6]{\frac{1}{20} \sum_{i=0}^{19} (\text{FD}_{10s+i}^u)^6} \quad (33)$$

$$d_{sym} = \sum_{u=0}^{B-1} \sqrt{\frac{1}{S^u} \sum_{s=0}^{S^u-1} (\text{PSQM}_s^u)^2} \quad (34)$$

where S^u is $\lfloor \frac{M^u}{10} \rfloor$. d_{asym} can also be found with similar averaging.

3.3. Joint SDR and PESQ optimization

To jointly maximize SDR and PESQ, a new loss function is defined by combining L_{SDR} and L_{PESQ} :

$$L_{\text{SDR-PESQ}} = L_{\text{SDR}} + \alpha L_{\text{PESQ}} \quad (35)$$

Another combined loss function is defined using MSE criterion instead of L_{PESQ} :

$$L_{\text{SDR-MSE}} = L_{\text{SDR}} + \alpha \sum_{u=0}^{B-1} \sum_{m=0}^{M-1} \sum_{k=0}^{K-1} (M_{m,k}^u |Y_{m,k}^u| - |X_{m,k}^u|)^2 \quad (36)$$

By comparing $L_{\text{SDR-MSE}}$ with $L_{\text{SDR-PESQ}}$, we can evaluate PESQ improvement from the proposed PESQ loss function over MSE criterion.

4. Experiments and Results

4.1. Experimental Settings

Table 1. Train and test sets sampled from QUT-NOISE-TIMIT. The notation is X-Y-N. X refers to noise type, Y is a recorded location for the noise and N is session number.

Train Set	CAFE-FOODCOURTB-1, CAFE-FOODCOURTB-2, CAR-WINDOWNB-1, CAR-WINDOWNM-2, HOME- KITCHEN-1, HOME-KITCHEN-2, REVERB-POOL1, REVERB-POOL2, STREET-CITY-1, STREET-CITY2
Test Set	CAFE-CAFE-1, CAR-WINUPB-1, HOME-LIVING-1, REVERB-CARPARK-1, STREET-KG-1

In order to evaluate the proposed denoising framework, we used the following three datasets:

CHIME-4 (Vincent et al., 2017): Simulated dataset is used for training and evaluation. It is synthesized by mixing Wall Street Journal (WSJ) corpus with noise sources from four different environments: bus, cafe, pedestrian area and street junction. Four noise conditions are applied to both train and development data. Moreover, simulated dataset has fixed SNR and therefore, it is relatively easy data to improve.

QUT-NOISE-TIMIT (Dean et al., 2010): QUT-NOISE-TIMIT corpus is created by mixing 5 different background noise sources with TIMIT clean speech (Garofolo et al., 1993). Unlike CHIME-4, the synthesized speech sequences provide wide range of SNR categories from -10dB to 15dB SNR. For training set, only -5 and 5 dB SNR data were used but test set contains all SNR ranges. The noise and location information used for train and test sets are summarized in Table 1.

VoiceBank-DEMAND (Valentini et al., 2016): 30 speakers selected from Voice Bank corpus (Veaux et al., 2013) were mixed with 10 noise types: 8 from Demand dataset (Thiemann et al., 2013) and 2 artificially generated one. Test set is generated with 5 noise types from Demand that does not coincide with those for training data. VoiceBank-DEMAND corpus was used to evaluate generative models such as SEGAN (Pascual et al., 2017), TF-GAN (Soni et al., 2018) and WAVENET (Rethage et al., 2018).

4.2. Model Comparison

Table 2. SDR and PESQ results between different denoising architectures on CHIME-4 corpus. The result for DNN* came from (Bando et al., 2018).

Model	G-L Iter.	Loss Type	SDR	PESQ
Noisy Input	-	-	5.80	1.267
OM-LSA	-	-	8.50	1.514
DNN*	-	IRM	10.93	-
CNN DAE	1	IAM	11.30	1.507
CNN DAE	10	IAM	11.21	1.491
CNN-BLSTM	1	IAM	11.91	1.822
CNN-BLSTM	10	IAM	12.06	1.829

Table 2 showed SDR and PESQ performance for various denoising networks based on CHIME-4 corpus. OM-LSA is a baseline statistical scheme that presented 2.7 dB SDR gain and 0.25 PESQ improvement. For neural network-based approaches, the author in (Bando et al., 2018) presented 10.93 dB SDR for 5-layer DNN. In this paper, two models were trained: CNN-based denoising autoencoder (DAE) and CNN-BLSTM. The generator architecture in (Pascual et al., 2017) was used for CNN-DAE. It presented SDR improvement over DNN model but PESQ performance is worse than OM-LSA. For CNN-BLSTM, both SDR and PESQ significantly improved, which is why we chose it as our model architecture.

Iterative Griffin-Lim algorithm (Griffin & Lim, 1984) was evaluated for CNN-DAE and CNN-BLSTM at the inference time. SDR and PESQ for two networks converged after 10 iterations. CNN-BLSTM showed 0.15 dB SDR gain from

Table 3. SDR and PESQ results on QUT-NOISE-TIMIT: Test set consists of 6 SNR ranges:-10, -5, 0, 5, 10, 15 dB. The highest SDR or PESQ scores for each SNR test data were highlighted with bold fonts.

Loss Type	SDR						PESQ					
	-10 dB	-5 dB	0 dB	5 dB	10 dB	15 dB	-10 dB	-5 dB	0 dB	5 dB	10 dB	15 dB
Noisy Input	-11.82	-7.33	-3.27	0.21	2.55	5.03	1.07	1.08	1.13	1.26	1.44	1.72
IAM	-3.23	0.49	2.79	4.63	5.74	7.52	1.29	1.47	1.66	1.88	2.07	2.30
PSM	-2.95	0.92	3.37	5.40	6.64	8.50	1.30	1.49	1.71	1.94	2.15	2.37
SNR	-2.79	1.36	3.70	5.68	6.18	8.44	1.29	1.46	1.68	1.93	2.14	2.38
SDR	-2.66	1.55	4.13	6.25	7.53	9.39	1.26	1.42	1.65	1.92	2.16	2.41
SDR-MSE	-2.53	1.57	4.10	6.31	7.60	9.43	1.29	1.47	1.68	1.93	2.15	2.39
SDR-PESQ	-2.31	1.80	4.36	6.51	7.79	9.65	1.43	1.65	1.89	2.16	2.35	2.54

10 iterations, on the other hand, CNN DAE showed 0.1 dB loss. Although iterative Griffin-Lim algorithm reduces spectra amplitude mismatch for each iteration, spectra phase also changes from update. Spectra phase update is not predictable. As shown in this experiment, sometimes, it is beneficial but in other case, it is not. Due to unstable SDR performance, iterative Griffin-Lim algorithm was not used in the inference time. Iterative Griffin-Lim in the training stage would be evaluated at the later section.

4.3. Main Results

Table 3 compared SDR and PESQ performance between different denoising methods on QUT-NOISE-TIMIT corpus. All the schemes were based on the same CNN-BLSTM model and trained with -5 and +5 dB SNR data as explained at Section 4.1. IAM and PSM are two spectra mask estimation schemes explained at Section 2.1. SDR refers L_{SDR} at Section 3.1 and SDR-MSE and SDR-PESQ correspond to $L_{\text{SDR-PESQ}}$ and $L_{\text{SDR-MSE}}$ at Section 3.3, respectively.

The proposed end-to-end scheme based on L_{SDR} showed significant SDR gain over spectra mask schemes for all SNR ranges. However, for PESQ, it did not show similar improvement due to metric mismatch. For example, PESQ performance degraded on the low SNR ranges such as -10, -5 and 0 dB over PSM.

Two proposed joint optimization schemes were evaluated. First, $L_{\text{SDR-MSE}}$ showed improvement on both SDR and PESQ metrics for the most of SNR ranges. However, the improvement is marginal and it still suffered from PESQ loss on low SNR ranges over PSM. Second, $L_{\text{SDR-PESQ}}$ loss function improved both SDR and PESQ metrics with large margin over all other schemes. By combining L_{PESQ} loss function with L_{SDR} , both SDR and PESQ performances were significantly improved.

At Section 3.1, we claimed MSE loss function cannot correctly maximize SDR. To evaluate this statement, we trained CNN-BLSTM with MSE criterion, which is the SNR en-

try in Table 1. Compared with L_{SDR} , SDR performance for SNR loss function degraded for all SNR ranges. One thing to note is that PESQ performance does not degrade. Therefore, this also showed that L_{SDR} or SNR loss functions couldn't correctly impact PESQ metric.

Table 4. SDR and PESQ results on CHIME-4

LOSS TYPE	SDR	PESQ
IAM	11.91	1.822
PSM	12.08	1.857
SDR	12.43	1.699
SDR-MSE	12.44	1.758
SDR-PESQ	12.59	1.953

Table 4 showed SDR and PESQ result on CHIME-4. The result is similar to QUT-NOISE-TIMIT. L_{SDR} presented significant SDR improvement but PESQ performance degraded. The proposed joint SDR and PESQ optimization presented the best performance both on SDR and PESQ metrics.

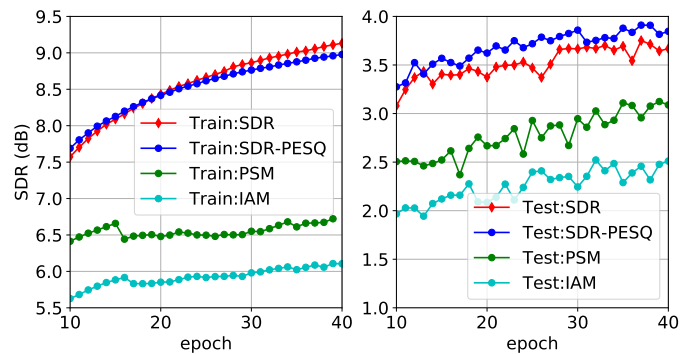


Figure 5. Train and test SDR curve comparison between different denoising schemes

The proposed joint optimization loss, $L_{\text{SDR-PESQ}}$ improved both SDR and PESQ even compared with L_{SDR} . It is logical

to guess L_{SDR} should present the best SDR performance. However, for both CHIME-4 and QUT-NOISE-TIMIT corpora, PESQ loss function in $L_{\text{SDR-PESQ}}$ was also helpful to improve SDR metric. The reason can be explained by train and test curves in Figure 5. The training SDR curve for L_{SDR} reached the highest value as expected but it showed the lower SDR on the test set than $L_{\text{SDR-PESQ}}$. Clearly, L_{PESQ} also acted as a regularizer to avoid overfitting. We tried other regularization terms such as L_1 and L_2 norms but L_{PESQ} was more effective to improve generalization to unseen data than other general regularization methods.

4.4. Comparison with Generative Models

Table 5. Evaluation on VoiceBank-DEMAND corpus: DCUnet-10 and DCUnet-20 are based on real-valued network (RMRn).

Models	CSIG	CBAK	COVL	PESQ	SSNR
Noisy Input	3.37	2.49	2.66	1.99	2.17
SEGAN	3.48	2.94	2.80	2.16	7.73
WAVENET	3.62	3.23	2.98	-	-
TF-GAN	3.80	3.12	3.14	2.53	-
DCUnet-10	3.70	3.22	3.10	2.52	9.40
DCUnet-20	4.12	3.47	3.51	2.87	9.96
WSDR	3.54	3.24	3.01	2.51	9.93
SDR-PESQ	4.09	3.54	3.55	3.01	10.44

Table 5 showed comparison with other generative models. All the results except our end-to-end model came from the original papers: SEGAN (Pascual et al., 2017), WAVENET (Rethage et al., 2018) and TF-GAN (Soni et al., 2018). CSIG, CBAK and COVL are objective measures where high value means better quality of speech (Hu & Loizou, 2008). CSIG is mean opinion score (MOS) of signal distortion, CBAK is MOS of background noise intrusiveness and COVL is MOS of the overall effect. SSNR is Segmental SNR defined in (Quackenbush, 1986).

The proposed SDR and PESQ joint optimization scheme outperformed all the generative models in all objective measures. Unfortunately, the original papers didn’t provide SDR metric. SSNR metric is similar to SDR but basically, SSNR is scale-sensitive metric and therefore, SDR loss function would not be optimal to maximize SSNR. Nevertheless, SSNR performance for the SDR-PESQ loss function showed significant gain over other generative models.

The results for DCUnet-10 and DCUnet-20 in Table 5 came from the recent paper (Choi et al., 2019). This paper suggested a couple of fancy ideas. One of main contributions was phase compensation scheme, which showed significant improvement on VoiceBank-DEMAND corpus. Our proposed joint optimization scheme was based on spectra amplitude estimation. However, it is not limited to real

mask estimation but can also enjoy phase compensation gain if applied. Therefore, the gain from complex mask should be removed for fair comparison. Fortunately, this paper provided its scheme based on real-valued network (RMRn), which were shown in Table 5. Our joint optimization scheme, $L_{\text{SDR-PESQ}}$ presented better performance on almost all the objective measures. In order to remove performance variation from model difference, a CNN-BLSTM model was also trained with the weighted SDR loss function proposed in this paper, which is WSDR in Table 5. It showed comparable performance to DCUnet-10. Compared with $L_{\text{SDR-PESQ}}$, it showed large loss especially for PESQ and SSNR.

4.5. Training with Iterative Griffin-Lim Algorithm

Table 6. SDR and PESQ evaluation of Iterative Griffin-Lim algorithm applied to joint SDR and PESQ optimization

Griffin-Lim Iteration	SDR	PESQ
1	12.59	1.953
2	11.59	1.679
3	12.35	1.949
4	11.61	1.638

K-MISI scheme for blind source separation (Wang et al., 2018) applied multiple STFT-ISTFT operations similar to iterative Griffin-Lim algorithm. It showed SDR improvement by increasing the number of iterations. We also applied iterative Griffin-Lim algorithm to our end-to-end joint optimization at the training stage. Table 6 showed SDR and PESQ performance for each Griffin-Lim iteration. Multiple iteration of Griffin-Lim algorithm only hurt SDR and PESQ performance unlike K-MISI. The key difference in K-MISI is that the reconstructed time-domain signal is redistributed between multiple sources for each iteration, which could provide substantial enhancement of source separation. For single source denoising problem, single iteration of Griffin-Lim algorithm presented the best performance.

5. Conclusion

In this paper, a new end-to-end multi-task denoising scheme was proposed. The proposed scheme resolved two issues addressed before: Spectra and Metric mismatches. First, two metric-based loss functions are defined: SDR and PESQ loss functions. Second, two newly defined loss functions are combined for joint SDR and PESQ optimization. Finally, the combined loss function is optimized based on the reconstructed time-domain signal after Griffin-Lim ISTFT in order to avoid metric mismatch. The experimental result presented that the proposed joint optimization scheme significantly improved SDR and PESQ performances over both spectra mask estimation schemes and generative models.

References

- Bando, Y., Mimura, M., Itoyama, K., Yoshii, K., and Kawahara, T. Statistical speech enhancement based on probabilistic integration of variational autoencoder and non-negative matrix factorization. In *2018 IEEE International Conference on Acoustics, Speech and Signal Processing (ICASSP)*, pp. 716–720. IEEE, 2018.
- Choi, H.-S., Kim, J., Huh, J., Kim, A., Ha, J.-W., and Lee, K. Phase-aware speech enhancement with deep complex u-net. *ICLR*, 2019.
- Cohen, I. and Berdugo, B. Speech enhancement for non-stationary noise environments. *Signal processing*, 81(11): 2403–2418, 2001.
- Dean, D. B., Sridharan, S., Vogt, R. J., and Mason, M. W. The qut-noise-timit corpus for the evaluation of voice activity detection algorithms. *Proceedings of Interspeech 2010*, 2010.
- Ephraim, Y. and Malah, D. Speech enhancement using a minimum-mean square error short-time spectral amplitude estimator. *IEEE Transactions on acoustics, speech, and signal processing*, 32(6):1109–1121, 1984.
- Ephraim, Y. and Malah, D. Speech enhancement using a minimum mean-square error log-spectral amplitude estimator. *IEEE transactions on acoustics, speech, and signal processing*, 33(2):443–445, 1985.
- Erdogan, H., Hershey, J. R., Watanabe, S., and Le Roux, J. Phase-sensitive and recognition-boosted speech separation using deep recurrent neural networks. In *Acoustics, Speech and Signal Processing (ICASSP), 2015 IEEE International Conference on*, pp. 708–712. IEEE, 2015.
- Garofolo, J. S., Lamel, L. F., Fisher, W. M., Fiscus, J. G., and Pallett, D. S. Darpa timit acoustic-phonetic continuous speech corpus cd-rom. nist speech disc 1-1.1. *NASA STI/Recon technical report n*, 93, 1993.
- Griffin, D. and Lim, J. Signal estimation from modified short-time fourier transform. *IEEE Transactions on Acoustics, Speech, and Signal Processing*, 32(2):236–243, 1984.
- Hu, Y. and Loizou, P. C. Evaluation of objective quality measures for speech enhancement. *IEEE Transactions on audio, speech, and language processing*, 16(1):229–238, 2008.
- Narayanan, A. and Wang, D. Ideal ratio mask estimation using deep neural networks for robust speech recognition. In *Acoustics, Speech and Signal Processing (ICASSP), 2013 IEEE International Conference on*, pp. 7092–7096. IEEE, 2013.
- Pascual, S., Bonafonte, A., and Serra, J. Segan: Speech enhancement generative adversarial network. *arXiv preprint arXiv:1703.09452*, 2017.
- Quackenbush, S. R. Objective measures of speech quality (subjective). 1986.
- Rethage, D., Pons, J., and Serra, X. A wavenet for speech denoising. In *2018 IEEE International Conference on Acoustics, Speech and Signal Processing (ICASSP)*, pp. 5069–5073. IEEE, 2018.
- Rix, A. W., Beerends, J. G., Hollier, M. P., and Hekstra, A. P. Perceptual evaluation of speech quality (pesq)-a new method for speech quality assessment of telephone networks and codecs. In *Acoustics, Speech, and Signal Processing, 2001. Proceedings.(ICASSP'01). 2001 IEEE International Conference on*, volume 2, pp. 749–752. IEEE, 2001.
- Roux, J. L., Wisdom, S., Erdogan, H., and Hershey, J. R. Sdr-half-baked or well done? *arXiv preprint arXiv:1811.02508*, 2018.
- Soni, M. H., Shah, N., and Patil, H. A. Time-frequency masking-based speech enhancement using generative adversarial network. 2018.
- Thiemann, J., Ito, N., and Vincent, E. The diverse environments multi-channel acoustic noise database: A database of multichannel environmental noise recordings. *The Journal of the Acoustical Society of America*, 133(5): 3591–3591, 2013.
- Valentini, C., Wang, X., Takaki, S., and Yamagishi, J. Investigating rnn-based speech enhancement methods for noise-robust text-to-speech. In *9th ISCA Speech Synthesis Workshop*, pp. 146–152, 2016.
- Veaux, C., Yamagishi, J., and King, S. The voice bank corpus: Design, collection and data analysis of a large regional accent speech database. In *Oriental COCODA held jointly with 2013 Conference on Asian Spoken Language Research and Evaluation (O-COCODA/CASLRE), 2013 International Conference*, pp. 1–4. IEEE, 2013.
- Vincent, E., Gribonval, R., and Févotte, C. Performance measurement in blind audio source separation. *IEEE transactions on audio, speech, and language processing*, 14(4):1462–1469, 2006.
- Vincent, E., Watanabe, S., Nugraha, A. A., Barker, J., and Marxer, R. An analysis of environment, microphone and data simulation mismatches in robust speech recognition. *Computer Speech & Language*, 46:535–557, 2017.

- Wang, Y., Narayanan, A., and Wang, D. On training targets for supervised speech separation. *IEEE/ACM Transactions on Audio, Speech and Language Processing (TASLP)*, 22(12):1849–1858, 2014.
- Wang, Z.-Q., Roux, J. L., Wang, D., and Hershey, J. R. End-to-end speech separation with unfolded iterative phase reconstruction. *arXiv preprint arXiv:1804.10204*, 2018.
- Weninger, F., Hershey, J. R., Le Roux, J., and Schuller, B. Discriminatively trained recurrent neural networks for single-channel speech separation. In *Proceedings 2nd IEEE Global Conference on Signal and Information Processing, GlobalSIP, Machine Learning Applications in Speech Processing Symposium, Atlanta, GA, USA, 2014*.
- Zwicker, E. and Feldtkeller, R. *Das Ohr als Nachrichtenempfänger*. Hirzel, 1967.